

A Tensor-based Technique for Structure-aware Image Inpainting

Adib Akl and Charles Yaacoub

*Faculty of Engineering, Holy Spirit University of Kaslik (USEK), Jounieh, Lebanon
{adibakl, charlesyaacoub}@usek.edu.lb*

Keywords: Image Inpainting, Orientation, Second-moment Matrix, Exemplar.

Abstract: Image inpainting is an active area of study in computer graphics, computer vision and image processing. Different image inpainting algorithms have been recently proposed. Most of them have shown their efficiency with different image types. However, failure cases still exist, especially when dealing with local image variations. This paper presents an image inpainting approach based on structure layer modeling, where this latter is represented by the second-moment matrix, also known as the structure tensor. The structure layer of the image is first inpainted using the non-parametric synthesis algorithm of Wei and Levoy, then the inpainted field of second-moment matrices is used to constrain the inpainting of the image itself. Results show that using the structural information, relevant local patterns can be better inpainted comparing to the standard intensity-based approach.

1 INTRODUCTION

Image inpainting is a dynamic research field with different applications. It is used in video animations, video completion, frames merging, image restoration, image extrapolation, image editing and video compression (Kwatra et al., 2003, Bargteil et al., 2006, Yamauchi et al., 2003, Winkenbach and Salesin, 1994). It is also used to describe the geometry of a surface, to remove undesired objects from images and videos and to fill missing regions (Bertalmio et al., 2000).

In the past decades, several image inpainting algorithms have been proposed. For instance, the image synthesis method of Paget and Longstaff (Paget and Longstaff, 1998) captures the local characteristics of an image into a statistical model describing the interaction between the pixels of this image. The Efros and Leung (Efros and Leung, 1999) approach generates the inpainted image by directly sampling new values from the input sample. The exemplar-based algorithms in (Criminisi et al., 2004) and (Aujol et al., 2009) consist in directly copying patches from the exemplar image. A method based on the graph cut technique, used to determine the patch region without choosing its size a-priori, is proposed in (Kwatra et al., 2003). Portilla and Simoncelli (Portilla and Simoncelli, 2000) rely on the wavelet transform used to parameterize the image by a set of statistics, at adjacent scales and

locations. A total variation inpainting model is proposed in (Chan and Shen, 2001). It is based on the theory of Euler-Lagrange and on anisotropic diffusion. The non-parametric image synthesis algorithm of Wei and Levoy (Wei and Levoy, 2000) models the image as a realization of a local and stationary random process.

It has been demonstrated that taking into consideration the structural information of an image can help in the synthesis of this image, especially in the case of local structural variations (Akl et al., 2014, Akl et al., 2015).

This paper presents a structure-based inpainting algorithm where the structure layer of the image, represented by the second-moment matrix field, is first inpainted, then the obtained structure field is used to help the image inpainting process. The proposed approach consists in adapting non-parametric image synthesis methods to the specificities of the second-moment matrix. More precisely, the algorithm of Wei and Levoy (Wei and Levoy, 2000) is used in the inpainting of the structure layer stage and in the inpainting process of the image itself.

The remainder of this paper is organized as follows: the second-moment matrix field computation is first reviewed in section 2. The proposed inpainting method is then detailed in section 3. Results are shown and discussed in section 4, and section 5 finally presents conclusions and perspectives of future work.

2 THE SECOND-MOMENT MATRIX

The second-moment matrix, also referred as the structure tensor, is a gradient-based matrix whose first eigenvector points in the direction of the greatest rate of increase of the scalar field (Bigun and Granlund, 1987, Akl and Iskandar, 2015, Akl and Iskandar, 2016). A second-moment matrix $SM(z)$ at image position z summarizes the dominant directions of the gradient in the neighbourhood of z . Therefore, it can be used to represent and to describe edges. In image processing, the second-moment matrix represents partial derivatives and it is commonly used to describe local patterns (Bigun and Granlund, 1987).

The second-moment matrix field SM of an image A is defined as the field of local covariance matrices of the partial derivatives of A , built using the gradient fields $[A_x, A_y]$ with:

$$A_x = A * G_x, \quad A_y = A * G_y, \quad (1)$$

where “*” represents convolution, G_x and G_y are isotropic Gaussian derivatives kernels.

The second-moment matrix field is computed as:

$$SM = \sigma_s * [A_x, A_y]^{\dagger} [A_x, A_y] \\ = \begin{pmatrix} SM^{xx} & SM^{xy} \\ SM^{xy} & SM^{yy} \end{pmatrix} = \begin{pmatrix} \sigma_s * A_x^2 & \sigma_s * A_x A_y \\ \sigma_s * A_x A_y & \sigma_s * A_y^2 \end{pmatrix}, \quad (2)$$

where $[\cdot]^{\dagger}$ is the transpose operator and σ_s is a weighting function – usually Gaussian – used to smooth the gradient fields, which makes them more robust to noise.

The second-moment matrix can be represented by an ellipse with its principle orientation, ranging between $-\pi/2$ and $\pi/2$, computed as:

$$\rho_{SM(z)} = \tan^{-1} \left(\frac{U_z^y}{U_z^x} \right), \quad (3)$$

where $U_z = [U_z^x \ U_z^y]$ is the first eigenvector of matrix $SM(z)$.

3 PROPOSED ALGORITHM

This section details the proposed image inpainting algorithm which consists of two stages; structure layer inpainting and image inpainting using the

inpainted structure, i.e. the second-moment matrix field.

For concision, we denote the missing area to be inpainted as “ MA ”, the reference from which the intensities are copied to the MA as “exemplar”, the image showing the MA and the exemplar as “input image” and the obtained image after inpainting as “output image” (Fig. 1).



Figure 1: Illustration of the inpainting principle. Left: input image showing the MA (missing area to be inpainted) marked as a black surface, and the exemplar (reference image from which the intensities are copied) contoured in red. Right: output image.

3.1 Structure Layer Inpainting

The inpainting process of the structure layer starts by computing the second-moment matrix field from the luminance component of the input image (cf. section 2). The luminance component is calculated as in (ITU-R, 2011). To ensure that the inpainted MA is locally similar to the neighbouring regions of the input image, the algorithm of Wei and Levoy is adapted to the specificities of the second-moment matrix as follows: the MA of the second-moment matrix field is first initialized as a random noise, i.e. second-moment matrices chosen randomly from the second-moment matrix field of the exemplar, then the neighbourhood (vector of matrices) of each second-moment matrix of the MA is captured, the neighbourhood of the second-moment matrix field of the exemplar having the best similarity with the current neighbourhood is determined, and its central structure tensor is copied to the current position in the MA , as illustrated in Fig. 2. In this latter, the second-moment matrix field is represented by its orientation image. The palette of orientations is shown on the right. Note that this palette is used for all the results that follow.

The similarity between two second-moment matrices at positions z_1 and z_2 is calculated using the square of the Euclidean distance as follows:

$$\Psi(SM(z_1), SM(z_2)) = \left(SM^{xx}(z_1) - SM^{xx}(z_2) \right)^2 + \left(SM^{yy}(z_1) - SM^{yy}(z_2) \right)^2 + 2 \left(SM^{xy}(z_1) - SM^{xy}(z_2) \right)^2, \quad (4)$$

and the similarity between two second-moment matrix neighbourhoods SM_1 and SM_2 is calculated using the Sum of Second-Moment Matrix Dissimilarity ($SSMD$):

$$SSMD(SM_1, SM_2) = \sum_{n=0}^{N-1} \Psi(SM_1(n), SM_2(n)), \quad (5)$$

where $SM_i(n)$ is the n^{th} second-moment matrix within the neighbourhood SM_i - $i \in \{1,2\}$ and N is the number of second-moment matrices in each neighbourhood.

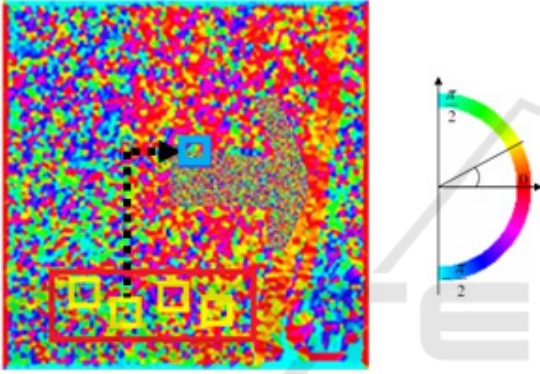


Figure 2: Second-moment matrix field inpainting. The most similar neighbourhood (yellow square) of the current neighbourhood (blue square) is searched for in the exemplar (contoured in red), and the corresponding matrix is copied to the target position in the MA . The palette used to represent the second-moment matrix field orientations is shown on the right.

Note that this synthesis process can be repeated iteratively in order to obtain an inpainted MA which is coherent with the remaining second-moment matrices of the input image, especially the neighbouring ones.

It is trivial that the neighbouring system (neighbour size and shape) and the scan type used in the inpainting process directly influence the quality of the inpainted MA . In this paper, the inpainting process starts by filling the outer border of the MA and ends at its center while using a square neighbourhood of size 9×9 . However, a random scan could avoid verbatim copies (Xu et al., 2000) i.e. when the inpainted MA seems more regular than neighbouring second-moment matrices of the input image.

3.2 Image Inpainting

The structure layer being inpainted, it will be used to help the inpainting of the output image. The inpainting process remains the same as the algorithm of Wei and Levoy, except that the neighbourhoods take into consideration the additional information provided by the inpainted second-moment matrix field.

More precisely, the image inpainting algorithm takes as inputs, the exemplar, its second-moment matrix field, the inpainted second-moment matrix field (cf. section 3.1) and the output image with its MA initialized by random noise (i.e. intensity values chosen randomly from the reference image). Then intensity values of the missing pixels of the MA are updated iteratively in order to ensure their local similarity with neighbouring pixels in the rest of the input image: the neighbourhood of every missing pixel of the MA is captured, the most similar neighbourhood is searched for in the exemplar and copied entirely to the target position in the MA . However, the underlying neighbourhoods have two components: an intensity component in the exemplar (A_2) and the MA of the output image (A_1), and a second-moment matrix component in the structure layers of the exemplar (SM_2) and the output image MA (SM_1) as shown in Fig. 3.

Note that the MA pixels update is patch-based (i.e. the most similar neighbourhood is entirely copied to the target position) and not pixel by pixel (i.e. the center value of the most similar neighbourhood is copied to the target position) as it is the case in the second-moment matrix field inpainting stage, in order to reduce the computational load of the inpainting process. In fact, this can be achieved without any blockiness effect, thanks to the additional structural information provided by the inpainted second-moment matrix field.

To measure the similarity between two neighbourhoods, we propose to combine the Sum of Second-Moment Matrix Dissimilarity ($SSMD$), used for the second-moment matrix component (cf. equation (5)), and the Sum-square Distance (SD), used for the intensity component:

$$\Phi = \alpha \cdot SD(A_1, A_2) + (1 - \alpha) \cdot SSMD(SM_1, SM_2), \quad (6)$$

where SM_1 and SM_2 are respectively the second-moment matrix components of the neighbourhoods in the inpainted second-moment matrix field of the MA and in the second-moment matrix field of the

exemplar, A_1 and A_2 are respectively the intensity components of the neighbourhoods in the MA and in the exemplar (Fig. 3), α is a weight factor ($0 \leq \alpha \leq 1$ since SD and $SSMD$ are normalized), and the Sum-square Distance (SD) is given by:

$$SD(A_1, A_2) = \sum_{n=0}^{N-1} (A_1(n) - A_2(n))^2 \quad (7)$$

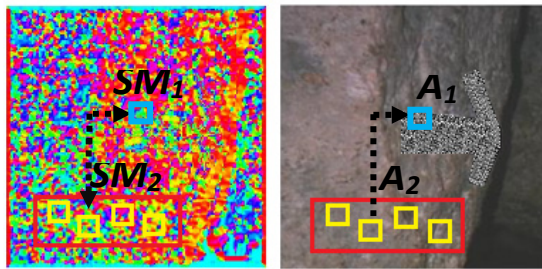


Figure 3: Illustration of the image inpainting process: for each current neighbourhood (A_1 in MA and SM_1 in its inpainted second-moment matrix field), the most similar neighbourhood (A_2 in the exemplar and SM_2 in its second-moment matrix field) is searched for, and the corresponding intensity component (A_2) is entirely copied to the target position (A_1).

Note that, when $\alpha = 1$, the second-moment matrix information is deactivated and a pure Wei and Levoy inpainting process is applied. On the contrary, when $\alpha = 0$, the intensity information is deactivated and the choice of the best similarity depends only on the second-moment matrix information.

The pseudocode of the whole inpainting algorithm is presented in Fig. 4.

It is important to mention that in both inpainting stages of the proposed algorithm, the Wei and Levoy method is used due to its versatility and its pixel based principle which proved its efficiency in the synthesis of different types of images. However, other image synthesis algorithms could also incorporate this structure-based approach.

4 RESULTS

In this section, some practical results are presented, evaluated and analyzed subjectively and objectively.

4.1 Qualitative Evaluation

Fig. 5 presents inpainting results obtained using the proposed algorithm on three different input images.

Structure Layer Inpainting

$SM \leftarrow$ SECOND-MOMENTMATRIXCALCULATION (A)

$MA^{SM} \leftarrow$ SMNOISEINITIALIZATION (SM)

loop through all positions zO of MA^{SM}

$z \leftarrow$ argmax {BESTSIMILARITY(SM_1^{zO} vs SM_2^z)}

$SM_1^{zO}(zO) \leftarrow SM_2^z(z)$

endloop

Image Inpainting

$MA \leftarrow$ NOISEINITIALIZATION (A)

loop through all positions zO of MA

$z \leftarrow$ argmax {BESTSIMILARITY(SM_1^{zO}, A_1^{zO}
vs SM_2^z, A_2^z)}

$A_1^{zO} \leftarrow A_2^z$

endloop

Figure 4: Pseudocode of the proposed inpainting algorithm.

Each result shows, from first to seventh row, the input image showing the missing area (marked as a black surface) and the exemplar (contoured in red), the structure layer of the input image, the inpainted structure layer obtained by the proposed approach, the output image obtained using the proposed algorithm with $\alpha = 1$ (pure Wei and Levoy inpainting), the output image obtained using the proposed approach with $\alpha = 0.5$, nearer view of the output images obtained with $\alpha = 1$ and $\alpha = 0.5$. As mentioned in section 3.1, square neighbourhoods of size 9×9 are used.

It can be seen in the first result that the proposed approach succeeds in well reproducing the structural information of the exemplar. The obtained orientation field of the structure layer does not present distortions nor edge effects. Therefore, the output image obtained with $\alpha = 0.5$ is of good quality and visually better than the one obtained with the intensity-based inpainting approach of Wei and Levoy.

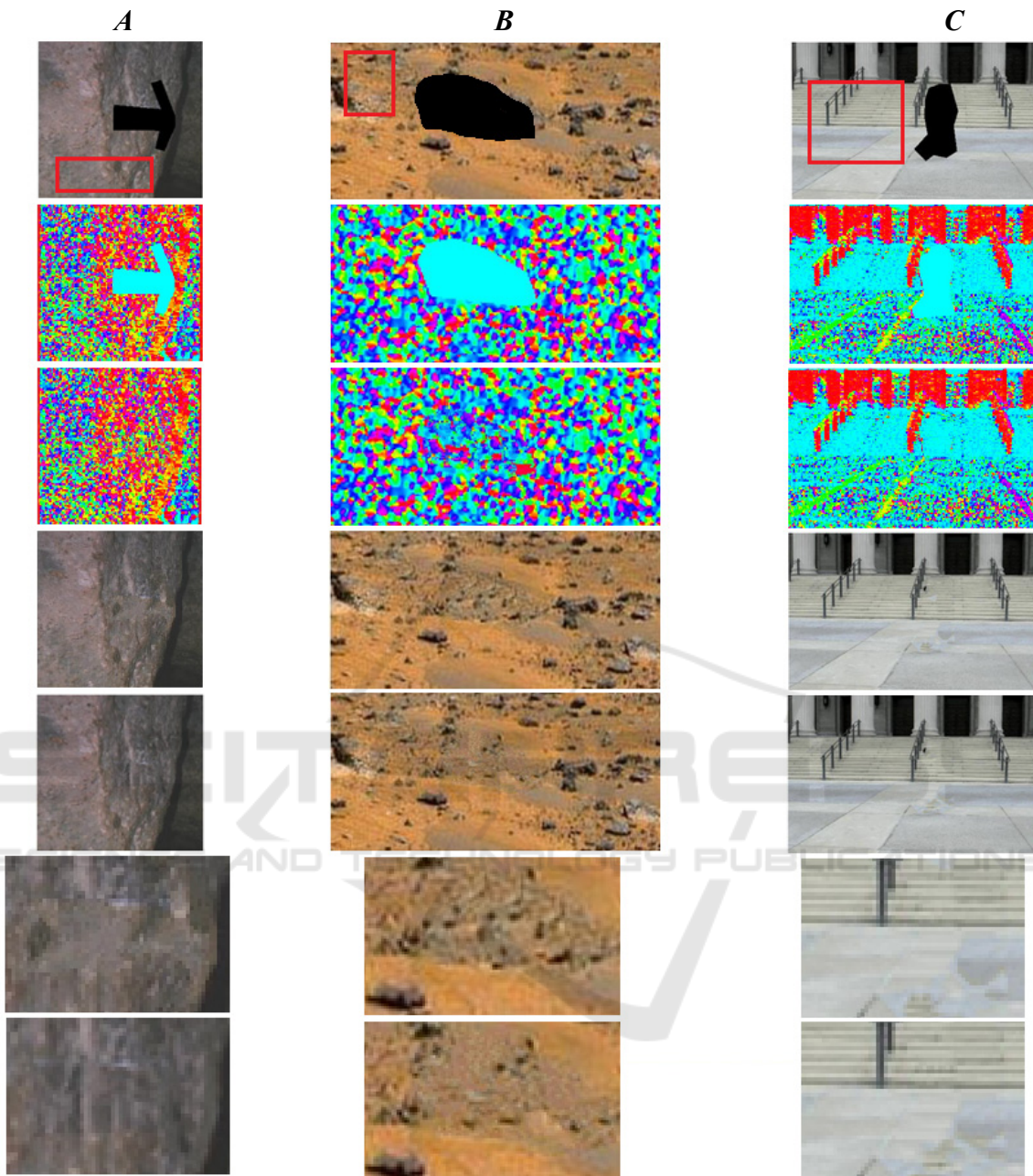


Figure 5: Inpainting results obtained by the proposed algorithm. For each result (1st to 7th row): input image, its structure layer orientation field, inpainted structure layer orientation field, output image obtained using the proposed approach while deactivating the structural information ($\alpha = 1$, pure Wei and Levoy inpainting), output image obtained using the proposed algorithm with $\alpha = 0.5$, nearer view of the output images obtained with $\alpha = 1$ and $\alpha = 0.5$.

The inpainted missing area obtained by this latter looks over smoothed and presents dynamics degradation. The same applies for the second result where the inpainted area obtained with $\alpha = 1$ appears more regular than the exemplar, i.e. repeated periodic patterns that do not exist in the exemplar

are present. In the third result, both output images are of acceptable quality.

4.2 Quantitative Evaluation

Besides the subjective qualitative evaluation presented in section 4.1, this section presents a

quantitative analysis of the results. It consists in comparing the histograms of intensity and orientations of the exemplar and the inpainted area by computing the Kullback and Leibler (Kullback and Leibler, 1951) divergence between them as follows:

$$KL(H_{MA} \parallel H_{exp}) = \sum_i H_{MA}(i) \log \frac{H_{MA}(i)}{H_{exp}(i)} + \sum_i H_{exp}(i) \log \frac{H_{exp}(i)}{H_{MA}(i)}, \quad (8)$$

where H_{MA} and H_{exp} are respectively the histograms of intensity (or orientation) of the missing area and the exemplar.

The Kullback and Leibler difference values obtained on the histograms of the output images of Fig. 5 are shown in Table 1.

Table 1: Objective results obtained on the images of Fig. 5.

Image	Intensity Histograms		Orientation Histograms	
	$\alpha = 1$	$\alpha = 0.5$	$\alpha = 1$	$\alpha = 0.5$
A	0.412	0.201	0.399	0.297
B	0.308	0.31	0.402	0.289
C	0.398	0.356	0.3	0.306

The objective evaluation of Table 1 generally confirms our subjective analysis. In result *A*, both intensity and orientation histogram differences are higher with $\alpha = 1$ than with $\alpha = 0.5$, which verifies that the dynamics of the inpainted missing area are distorted with the pure Wei and Levoy inpainting. The high orientation histogram difference (0.402) in result *B* is due to the undesired repetitive patterns shown in the inpainted area with $\alpha = 1$. Finally, the success of both, Wei and Levoy's algorithm and the proposed approach, in leading to output images of roughly similar quality, is verified in the last row of Table 1.

5 CONCLUSIONS

We have proposed an image inpainting algorithm which consists in first inpainting the structure layer of the image, then using it to constrain the inpainting process of the image. The proposed approach relies on adapting the algorithm of Wei and Levoy to the specificities of the second-moment matrix. The obtained results quality was highly encouraging, in terms of dynamics and structures preservation, and

proved that using the structure layer in the inpainting process could be advantageous comparing to pure intensity-based approaches.

However, using other non-parametric methods than Wei and Levoy, and evaluating their efficiency in the structure and image inpainting processes, is of our interest. We also aim at comparing the performance of the proposed algorithm with several existing inpainting methods, using a large database. In addition, we aim at reinforcing the use of the proposed approach with different inpainting scan types, different neighbourhood shapes and size. Finally, it is necessary to consolidate the proposed objective evaluation using second order statistics, such as the autocorrelation, for example.

ACKNOWLEDGMENT

This work has been partly supported by a research grant from the Higher Center for Research at the Holy Spirit University of Kaslik (USEK), Lebanon.

REFERENCES

- Kwatra, V., Schödl, A., Essa, I., Turk, G., Bobick, A., 2003. "Graphcut Textures: Image and Video Synthesis Using Graph Cuts," *Proc. of ACM SIGGRAPH*, pp. 277-286.
- Bargteil, A. W., Sin, F., Michaels, J. E., Goktekin, T. G., O'Brien, J. F., 2006. "A Texture Synthesis Method for Liquid Animations," *Proc. ACM SIGGRAPH/Eurographics Symposium on Computer Animation*, Vienna, Austria, September 2-4.
- Yamauchi, H., Haber, J., Seidel, H-P., 2003. "Image restoration using multiresolution texture synthesis and image inpainting," *Proc. Int. Conf. Comput. Graph.*
- Winkenbach, G., Salesin, D. H., 1994. "Computer-generated pen-and-ink illustration," *Proc. of SIGGRAPH 94*, pp. 91-100, Orlando, Florida.
- Bertalmio, M., Sapiro, G., Caselles, V., Ballester, C., 2000. "Image inpainting," *Proc. of the 27th annual conference on Computer graphics and interactive techniques*, pp. 417-424.
- Akl, A., Yaacoub, C., Donias, M., Da Costa, J.-P., Germain, C., 2015. Texture Synthesis Using the Structure Tensor. *IEEE Transactions on Image Processing*, 24 (11), art. no. 7163318, pp. 4082-4095.
- Paget, R., Longstaff, I.D., 1998. "Texture synthesis via a non causal nonparametric multiscale markov random field," *IEEE Trans. on Image Processing*, vol. 7(6), pp. 925-931.
- Efros, A., Leung, T., 1999. "Texture synthesis by non-parametric sampling," *International Conference on Computer Vision*, vol. 2, pp. 1033-1038.

- Chan, T., Shen, J., 2001. "Non-texture inpainting by curvature-driven diffusions," *J. Visual Comm. Image Rep.*
- Wei, L.-Y., Levoy, M., 2000. "Fast texture synthesis using tree-structured vector quantization," *Proc. of ACM SIGGRAPH 2000*, pp. 479-488.
- Portilla, J., Simoncelli, E.P., 2000. "A Parametric Texture Model based on Joint Statistics of Complex Wavelet Coefficients," *Int'l Journal of Computer Vision*, vol.40(1), pp. 49-71.
- Akl, A., Yaacoub, C., Donias, M., Da Costa, J.-P., Germain, C., 2015. Two-stage color texture synthesis using the structure tensor field. GRAPP 2015 - 10th International Conference on Computer Graphics Theory and Applications; VISIGRAPP, Proceedings, pp. 182-188.
- Bigun, J., Granlund, G., 1987. "Optimal Orientation Detection of Linear Symmetry," *International Conference on Computer Vision, ICCV*, (London). Piscataway: IEEE Computer Society Press, Piscataway. pp. 433-438.
- Aujol, J., Ladjal, S., Masnou, S., 2009. "Exemplar-based inpainting from a variational point of view," *SIAM Journal on Mathematical Analysis*.
- Akl, A., Yaacoub, C., Donias, M., Da Costa, J.-P., Germain, C., 2014. Structure tensor based synthesis of directional textures for virtual material design. 2014 IEEE International Conference on Image Processing, ICIP 2014, art. no. 7025986, pp. 4867-4871.
- ITU-R Recommendation BT.601-7, "Studio encoding parameters of digital television for standard 4:3 and wide screen 16:9 aspect ratios," ITU-R, Mar. 2011.
- Xu, Y.Q., Guo, B., Shum, H., 2000. "Chaos mosaic: Fast and memory efficient texture synthesis," *In Tech. Rep. MSRTR-2000-32*, Microsoft Research.
- Akl, A., Iskandar, J., 2015. Structure tensor regularization for texture analysis. 5th International Conference on Image Processing, Theory, Tools and Applications 2015, IPTA 2015, art. no. 7367217, pp. 592-596.
- Criminisi, A., Pérez, P., Toyama, K., 2004. "Region filling and object removal by exemplar-based image inpainting," *Microsoft Research*, Cambridge (UK) and Redmond (US).
- Kullback, S., Leibler, R.A., 1951. "On information and sufficiency," *Ann. Math. Statist.*, vol. 22(1), pp. 79-86.
- Akl, A., Iskandar, J., 2016. Second-moment matrix adaptation for local orientation estimation. International Conference on Systems, Signals, and Image Processing, 2016-June.